Original

Schille, C.; Schweizer, E.; Hort, N.; Reichel, H.-P.; Geis-Gerstorfer, J.:

Zone coulometry and ion-release analysis of degradable magnesium alloys

In: Emerging Materials Research (2013) ICE Publishing

DOI: 10.1680/emr.13.00023

Emerging Materials Research
Volume 2 Issue EMR5
Zone coulometry and ion-release analysis of degradable magnesium alloys
Schille, Schweizer, Hort, Reichel and Geis-Gerstorfer

Pages 248–262 http://dx.doi.org/10.1680/emr.13.00023
Themed Issue Research Paper
Received 27/05/2013 Accepted 18/09/2013
Published online 21/09/2013
Keywords: alloys/biomaterials/corrosion

ice | science

ice Institution of Civil Engineers publishing

Zone coulometry and ion-release analysis of degradable magnesium alloys

Christine Schille*
Technical assistant of physics, Dental Clinic, Section Medical Materials and Technology, University Hospital of Tuebingen, Tuebingen, Germany

Ernst Schweizer
Technical assistant of chemistry, Dental Clinic, Section Medical Materials and Technology, University Hospital of Tuebingen, Tuebingen, Germany

Norbert Hort Dr. Ing.
Head of department magnesium processing, Magnesium Innovation Center, Helmholtz-Zentrum Geesthacht, Geesthacht, Germany

Heinz-Peter Reichel Dipl.-Ing.
General manager, Weisensee Warmpressteile GmbH, Eichenzell, Germany

Jürgen Geis-Gerstorfer Prof. Dr. rer. nat., Dipl. Ing.
Chairman of Section Medical Materials and Technology, University Hospital of Tuebingen, Tuebingen, Germany

Zone coulometry and determination of ion release of an electrolyte from anodic polarization measurements are the established calculation modes for the electrochemical behavior of dental and biomedical alloys. The aim of the study was to compare the electrochemical corrosion behavior of six different experimental magnesium alloys without manganese using artificial plasma (AP) and in phosphate-buffered saline (PBS^-) as simulated body fluids through anodic polarization measurements. In addition, determination of the magnesium release of the electrolytes was performed using inductively coupled plasma optical emission spectrometry and zone coulometry. Six specimens were prepared from each alloy. Anodic polarization measurements ranging from –150 mV ~E_{corr} to –1200 mV were performed with both of the electrolytes. From each measurement, corrosion current density, the breakdown or pitting potential and its corresponding current density, zero potential, the polarization resistance, the corrosion rate were calculated. The magnesium release of the electrolytes was compared with the calculated values using Faraday's law. For zone coulometry, five different trials were completed, and the electrical charge was calculated for each potential range of all magnesium alloys tested and for both electrolytes. Lower corrosion values were found in AP than in PBS^- for all measurements. However, the rankings of the alloys are similar in both the electrolytes. Zone coulometry using small potential ranges and determination of ion release can be additional evaluation tools for magnesium alloys.

1. Introduction

Magnesium alloys that are used as bone-replacement material are expected to remain in the body until the bone-healing process is completed, which takes approximately 6 months. In addition, the magnesium alloys are expected to degrade during the bone-healing process. As the magnesium alloys dissolve over 6 months, new bone tissue assumes the function of the bone-replacement material. On the basis of the mechanical characteristics, the magnesium alloys had an elastic modulus (45 GPa) similar to bone (54 GPa). However, an issue for magnesium alloys is their rapid degradation *in vivo* and *in vitro*.[1–3]

To test the degradation behavior *in vitro*, various corrosion measurements using magnesium alloys in different electrolytes were performed. There are several different simulated body fluids (SBF) for the *in vitro* testing of magnesium alloys.[4–8] Artificial plasma (AP) can be used to simulate blood. AP has an HCO_3– ion concentration similar to that of blood, and this property of AP, similar to other electrolytes (Hank, Ringer solution), is responsible for the improved corrosion resistance in magnesium alloys.[6,7]

For the characterization of the *in vitro* corrosion behavior of magnesium alloys, various techniques, including open-circuit potential (E_{corr}) and anodic polarization measurements, electrochemical impedance spectroscopy and the immersion test, were performed using different electrolytes. The composition of the magnesium alloys and the identity of the electrolyte affected the corrosion results. On the basis of the anodic polarization measurements, parameters such as the corrosion current density (i_{corr}), the breakdown or pitting potential (E_p) and its corresponding current density (i_p), the polarization resistance (R_p), the corrosion rate (CR) and the zero potential (E_z) were calculated. In addition, the open-circuit potential E_{corr} was calculated from the open-circuit potential measurements.[7,9] When corrosion measurements

***Corresponding author e-mail address:** christine.schille@med.uni-tuebingen.de

are performed on magnesium alloys, corrosion processes begin immediately after immersion in a solution. This manifests itself, especially with uncoated magnesium in salt solution by formation a magnesium hydroxide layer and hydrogen bubbles. As this process continues and no immediate passivation of the surface occurs, no equilibrium of potential exists when starting the anodic polarization measurement.

The formation of hydrogen on the magnesium alloys proceeds according to the reaction, $Mg + 2H_2O \rightarrow Mg(OH)_2 + H_2$. This formation is the beginning of the degradation process during corrosion measurements; therefore, not all types of corrosion measurements that are typically used with biomedical or dental alloys can be performed. Different measurements were made to collect and calculate the hydrogen bubbles as additional mass loss during the corrosion measurements using a funnel and a burette.[8,10,11] The hydrogen evolution test collects the hydrogen bubbles that result during the immersion test.[11] Shi *et al*. used special samples and collected hydrogen bubbles during the Tafel plot measurements. The calculated CR from a special equation was compared with the calculated CR from the electrochemical data.[8,10] Differences were found between the calculation of the CR obtained from the immersion test and from i_{corr} data obtained using the electrochemical test. Shi *et al*. reported difficulties in describing the corrosion behavior of magnesium alloys using anodic polarization measurements. Therefore, there is a need to consider other methods such as zone coulometry in combination with the analytical determination of ion release into the electrolyte during anodic polarization. Both are well-established methods for the evaluation of dental alloy corrosion and can be performed in addition to corrosion measurements, according to ISO 10271.[9] For the quantification of ion release, the electrolyte can be analyzed using ICP-OES (inductively coupled plasma optical emission spectrometry), inductively coupled plasma mass spectrometry (ICP-MS) or atomic absorption spectroscopy. The analytically determined ion release can be compared with the calculated ion release using Faraday's law according to the equation $m = [Q \times M] / [z \times F]$, where Q is the electrical charge of the entire anodic polarization plot calculated using area integration in coulomb per square centimeter, M is the equivalent weight of the analyzed element in gram per mole, z is the number of electrons and F is Faraday's constant, which is 96486·70 As/mol. Nagayama *et al*. determined the electrical charges from the entire anodic portion of the anodic polarization plots of different dental alloys, and the ion release of the main element was calculated using Faraday's law. The electrolyte was analyzed using ICP-MS and the analyzed ion release was compared with the calculated ion release. A good correlation was found between the analytical and the calculated ion release.[12] For zone coulometry, the calculation of the total electrical charge of an anodic polarization plot using integration is the basis for dividing the anodic polarization plot into zones. The calculation of the electrical charge is based on the equation $Q = i \times t$, where i is the current density measured in ampere per square centimeter, and t is the time measured in seconds calculated using area integration. The scan rate affects the results of the calculated electrical charge. Another effect is from E_z, which is different for each alloy and electrolyte. The difference between E_z and E_{end} describes the length of the anodic component where dissolution occurs. Reclaru *et al*. and Maranche *et al*. evaluated different dental alloys by calculating the electrical charges of anodic polarization using integration. Reclaru and Maranche divided the anodic polarization plot into three different regions and calculated the electrical charge of each region. Reclaru divided the anodic polarization plots of different dental alloys from −300 to +300 mV (region 1), 300–700 mV (region 2) and 700–1000 mV (region 3). In the corrosion study from Maranche, region 1 was from E_z to 300 mV, region 2 was from E_z to 700 mV and region 3 was from E_z to 900 mV. An example of a schematic view of an experimental CoCr alloy is shown in Figure 1.[13] Reclaru divided the anodic polarization plot into a symmetrical region of zero potential, the total passive region and the total region of breakdown by evaluating each region completely. Maranche began every region at E_z, and the regions ended before the passive region, at the end of passive region or at the beginning of a breakdown and during a breakdown. Using these three investigations and this calculation, the corrosion behaviors of the dental and biomedical alloys could be categorized.[14,15] Zone coulometry using anodic polarization plots is an easy method, which can be performed using the electrochemical corrosion software of a potentiostat. Currently, Reclaru uses zone coulometric analysis as a standardized calculation parameter from anodic polarization measurements to answer different questions regarding the corrosion of dental and biomedical alloys.[16–19] Many corrosion measurements have been performed to evaluate the corrosion behavior of dental and biomedical alloys. The corrosion studies performed by Reclaru and Maranche omitted the calculation of mass loss using Faraday's law and a comparison with the analytical data of the electrolyte. To investigate the corrosion of CoCr alloys with different chromium contents, the electrical charge was calculated according to Reclaru and Maranche, and the results were compared with the analytical data. The best relationship between the analytical and the calculated mass loss of cobalt was found with electrical charges ranging from E_z to 900 mV.[13]

Zone coulometry provides additional information on the section of the anodic polarization plot where corrosion occurs. It is possible to calculate sections of the chosen regions relative to the total electrical charge using zone coulometry. However, it can be difficult to determine new zones for a new material. The corrosion of magnesium alloys occurs in a different potential range similar to those for dental or biomedical alloys. Because of their rapid degradation, most magnesium alloys have a small or nonexistent passive region. A breakdown potential generally occurs at less than 100 mV after E_z. The degradation potential of magnesium alloys starts at −1200 mV.[20] Calculation of the electrical charge from the anodic polarization plots was not found in corrosion investigations

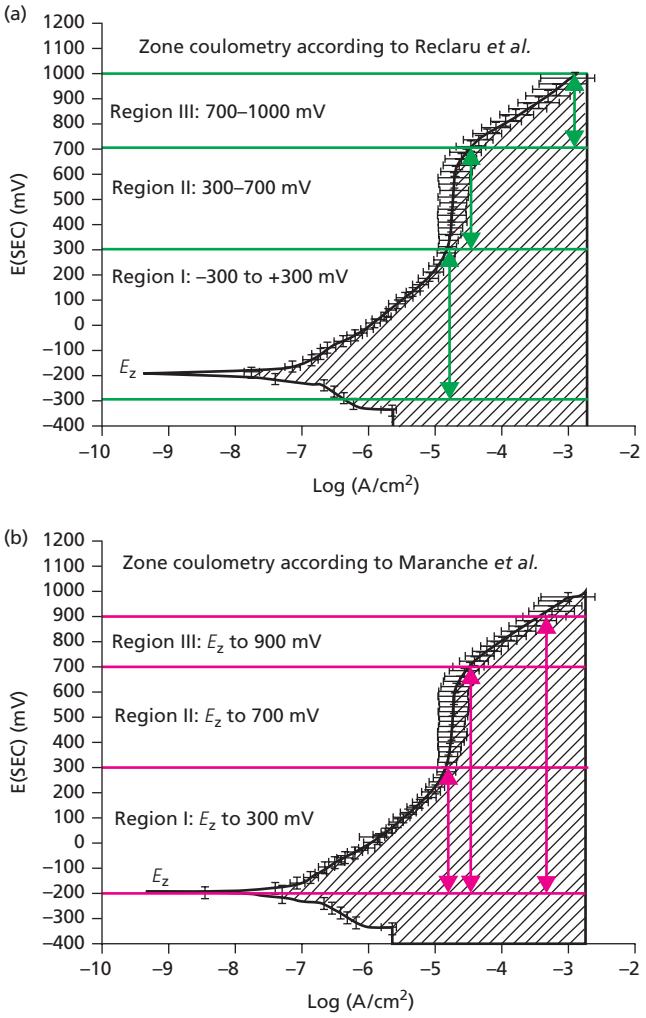

Figure 1. Schematic view of zone coulometry according to (a) Reclaru and (b) Maranche shown with an anodic polarization plot of an experimental CoCr alloy.[23]

of magnesium alloys in combination with ion-release analysis after anodic polarization measurements.[20,21]

1.1 Aim of the study

Usually, the electrochemical corrosion behavior of magnesium alloy was measured and evaluated with conventional anodic polarization measurement parameters. The aim of this study was to determine whether other evaluation tools can be used to characterize the electrochemical behavior of magnesium alloys from anodic polarization measurements. In this investigation, two additional tools were tested: the zone coulometry according to Reclaru and Maranche with five different trials of potential ranges, which were adjusted to the corrosion behavior of magnesium alloys and the determination of magnesium release in the electrolytes. Both additional tools are established tools for corrosion measurements of dental alloys and until now not used together with magnesium alloys

2. Materials and methods

2.1 Materials

Six highly pure experimental magnesium alloys were used in this investigation. The alloys were Mg1Zn, Mg4Y, Mg3Al, Mg9Al, Mg3Al1Zn and Mg9Al1Zn. They possess a composition similar to the magnesium alloys on the market, such as AZ31 and AZ91. However, they do not contain manganese. The composition of these alloys is shown in Table 1.[22]

Phosphate-buffered saline (PBS^-) (DPBS, Gibco, Invitrogen No. 190–146; Life Technologies GmbH, Darmstadt, Germany) and AP were used as SBF. PBS^- was a complete prepared solution that contained 8·0 g/l of sodium chloride, 2·160 g/l of sodium phosphate dibasic, 0·2 g/l of potassium chloride and 0·2 g/l of potassium phosphate monobasic. The composition of the modified AP contained 6·80 g/l of sodium chloride, 0·2 g/l of calcium dichloride, 0·4 g/l of potassium chloride, 2·20 g/l of sodium hydrogen carbonate, 0·126 g/l of disodium phosphate and 0·026 g/l of sodium dihydrogen phosphate (magnesium sulfate was not used). The pH values of the PBS^- and AP were 7·2 and 7·6, respectively.

2.2 Methods

Six specimens (discs with a diameter of 10 mm, thickness 1 mm) were prepared from each alloy. After grinding in ethanol with SiC 1200 and cleaning with ethanol in an ultrasonic bath for 5 min, each specimen was placed in a corrosion cell, which was filled with 100 ml of electrolyte (37°C) and exposed to air without stirring the electrolyte. All measurements were started immediately. For each specimen and both electrolytes, the anodic polarization measurements ranging from –150 mV ~E_{corr} to –500 mV (Ref) were performed at a scan rate of 1 mV/s (Potentiostat: PAR 273A, Software: M352, EG&G; AMETEK GmbH, Meerbusch, Germany). From each measurement, the i_{corr}, E_p, i_p, E_z, R_p and CR values were calculated according to ASTM G5.[23] To calculate i_{corr}, each semilogarithmic version of the anodic polarization plot was zoomed to ±250 mV ~E_z, and the linear regression cross-points of the anodic and cathodic sections were determined. E_p and the i_p were determined using the cross-point of the linear regression from the passive and the transpassive sections. To calculate R_p, the linear version of the anodic polarization plot was used. Each plot was zoomed to ±20 mV ~E_z, and the R_p was determined using the slope of linear regression. E_z is the potential at the transition between the anodic and cathodic section, and the current density was not measured. The CR (millimeter per year) was calculated using the equation $CR = [M \times t \times i_{corr} / n \times F \times \rho] \times 10$, where M is the equivalent weight of magnesium (24·31 g/mol), t is 3600×24×365 (s), n is the number of electrons (n = 2), F is 96485 As/mol and ρ is the density of magnesium (1·74 g/cm³). If the calculation of the CR was valid according to Stearn-Geary,

then the $1/R_p$–i_{corr} plots were created according to Grajower.[24] The magnesium releases for each electrolyte and all magnesium alloys tested were analyzed and calculated to the area of the specimen after each measurement. From the 100 ml of electrolyte, which was used for each measurement, four aliquots of 10 ml were taken (a total of 150 aliquots). Each aliquot was placed into a polypropylene tube and analyzed using ICP-OES (Optima 4300 DV, Perkin Elmer, Rodgau, Germany). The analytical magnesium release was compared with the calculated mass loss of magnesium using Faraday's law. The electrical charge of each anodic polarization measurement was calculated (Software: M352, EG&G, AMETEK GmbH, Meerbusch, Germany) from E_z to −500 mV (reference). The magnesium release was calculated using the equation $m = [Q \times M] / [z \times F]$, where M_{Mg} is 24·305 g/mol, z is 2, F is 96500 As/mol and Q is the electrical charge from the anodic polarization measurements. Two calculations modes were applied: With version 1, the electrical charge of the whole anodic polarization measurement was determined by integration and with version 2, the electrical charge was calculated based on $i \times t$ after 900 s. A Student's t-test ($p < 0{\cdot}05$) was performed on the electrochemical and analytical results. For zone coulometry, different potential ranges were determined, and the electrical charge was calculated for each magnesium alloy tested using both electrolytes. The choice of the potential ranges is shown in Table 2. The entire anodic polarization plot was covered using trials 1 and 2. Trials 3–5 relate to the initial corrosion behavior, which is clinically relevant. Using trials 1 and 2, the potential of each zone was increased in 100-mV steps (*i*) relative to E_z[14] and (*ii*) in absolute numbers.[15] Because the 100-mV steps were too large, further measurements were made using smaller potential steps ranging from 10 to 50 mV (trials 3–5). Following Maranche, the coulometric zones were calculated from E_z, which is the starting potential, to different E_{end}, including −1500, −1400, −1300 and −1200 mV (trial 1). Following Reclaru, the starting potential was −1600 mV, and the electrical charge in milli-Coulomb per square centimeter was stepwise calculated every 100 mV up to −1200 mV (trial 2) for zone coulometry. To obtain information regarding the initial corrosion process, three different potential ranges were chosen in the region of E_z. In trial 3, the cathodic and anodic portions of the anodic polarization plot were chosen symmetrically, and the electrical charge was calculated stepwise from ±10 mV ~E_z to ±50 mV ~E_z. For trial 4, E_z was the starting potential, and a stepwise increase of the potential from 10 up to 40 mV ~E_z was selected; the electrical charge that is represented

Magnesium alloys	Aluminum	Zinc	Yttrium	Neodymium	Iron	Copper	Nickel	Silicon	Magnesium
MgZn1	—	0·966	—	—	0·00275	0·00373	0·00206	0·0316	Balance
MgY4	—	—	4·95	—	0·00576	0·00419	<0·00020	0·0339	Balance
MgAl3	3·07	—	—	—	0·00311	0·00202	0·00096	0·0201	Balance
MgAl3Zn1	3·01	1·01	—	—	0·00387	0·00249	0·00106	0·0332	Balance
MgAl9	8·43	—	—	—	0·00152	0·00295	0·00063	0·0154	Balance
MgAl9Zn1	9·03	1·16	—	0·00503	0·00503	0·00363	0·00081	0·0229	Balance

The values are measured in weight per cent using Spektrolab M (Spektro, Kleve, Germany).

Table 1. Composition of the magnesium alloys.

Trial 1	Trial 2	Trial 3	Trial 4	Trial 5
E_z to −1500 mV	−1600 to −1500 mV	±10 mV ~E_z	E_z to +10 mV	−50 mV ~E_z to +10 mV
E_z to −1400 mV	−1500 to −1400 mV	± 20 mV ~E_z	E_z to +20 mV	−50 mV ~E_z to +20 mV
E_z to −1300 mV	−1400 to −1300 mV	± 30 mV ~E_z	E_z to +30 mV	−50 mV ~E_z to +30 mV
E_z to −1200 mV	−1300 to −1200 mV	± 40 mV ~E_z	E_z to +40 mV	−50 mV ~E_z to +40 mV
		± 50 mV ~E_z	E_z to +50 mV	
Results shown in Figure 4	Results shown in Figure 5	Results shown in Figure 6	Results shown in Figure 7	Results shown in Figure 8

E_z, zero potential.

Table 2. Choice of potential ranges for zone coulometry.

as milli-Coulomb per square centimeter was calculated for every potential range. For trial 5, –50 mV ~E_z was the starting potential, and the electrical charge, represented in milli-Coulomb per square centimeter, was calculated stepwise from 10 to 40 mV ~E_z. Bar diagrams of the calculated electrical charges for each alloy depending on the electrolyte were created for each trial. Because the degradation process began in the anodic section and most potential zones for zone coulometry started at E_z, which was different for each magnesium alloy and electrolyte, the anodic immersion time was calculated for each magnesium alloy and electrolyte based on the difference between E_z and E_{end}, which depends on the potential scan rate.

3. Results

3.1 Anodic polarization measurements

Figure 2(a)–2(f) shows the mean curves of the anodic polarization measurement plots for each magnesium alloy tested with each electrolyte. The calculated i_{corr}, R_p, E_p, i_p and the CR from the anodic polarization measurements for both electrolytes are presented in Table 3. Using both types of electrochemical corrosion measurements, all of the magnesium alloys tested showed better corrosion values in AP than the values in PBS$^-$. In AP, all magnesium alloys showed lower i_{corr} values than in PBS$^-$. A difference between the magnesium with a rare earth content and that containing aluminum was observed using all calculated parameters. The i_{corr} values of the Mg1Zn and Mg4Y were less than 100 nA/cm^2 in PBS$^-$ and less than 20 µA/cm^2 in the AP. An increase in R_p values (greater than 1000 Ωcm^2) was observed using these two alloys in the AP. The two alloys showed a small passive layer, and a breakdown potential could be calculated. The i_p values were significantly lower in AP. However, the formation of the breakdown potential and the passive layer could be observed only with Mg1Zn in PBS$^-$. All magnesium alloys containing aluminum showed no breakdown potential in both electrolytes. The i_{corr} values of all magnesium alloys with aluminum content were lower in the AP compared with PBS$^-$. The R_p values of these alloys were less than 500 Ωcm^2 in both electrolytes and were only slightly reduced in AP. The addition of zinc could be compared with aluminum in both electrolytes using the parameters i_{corr}, E_{corr} and R_p. The addition of zinc increases the E_{corr} values to improved potential values in both electrolytes. The R_p values of MgAl9Zn1 were similar in both electrolytes and showed the highest values with magnesium alloys containing aluminum and zinc. The i_{corr} value of the MgAl9Zn1 alloy decreased in both electrolytes. In the AP, the i_{corr} value and the calculated CR of MgAl9Zn1 showed values similar to those for MgZn1 and Mg4Y. E_z was ca. 100 mV above −1500 mV for the magnesium alloys MgZn1 and MgY4. The other alloys were tested at −1500 mV. MgAl9 was the only alloy with an E_z greater than −1500 mV. Similar results were found for the calculated anodic immersion time. MgZn1 and MgY4 showed the longest time, and MgAl9 showed the shortest time for both electrolytes (Table 3).

3.2 Magnesium release of the electrolytes from the anodic polarization measurements

The results of the magnesium release (analyzed by ICP-OES/calculated by Faraday's law) in both electrolytes and in all magnesium alloys tested are shown in Figure 3. The significant values were obtained using Student's t-test ($p < 0{\cdot}05$).

Using the electrical charge from the whole anodic polarization plot (calculation version 1), the analytical magnesium release was higher than the calculated magnesium release for all magnesium alloys tested in PBS$^-$. However, in AP, a similar relationship was only found with the magnesium alloys containing aluminum and not for MgZn1 and MgY4. The lowest magnesium release (analyzed/calculated) was found for MgAl9Zn1, and the highest was for MgZn1 in PBS$^-$. The ranking is different in AP; the highest analytical values were found for MgAl3Zn1, and the lowest for MgY4. In contrast, the lowest calculated data were obtained for MgAl9, and the highest calculated magnesium release was observed for MgZn1. In the analytical data from ICP-OES, aluminum release was also found for MgAl9 and MgAl3Zn1 in AP. Magnesium release could only be measured from other magnesium alloys. Therefore, the total ion release for MgAl9 and MgAl3Zn1 is higher.

An independent t-test ($p < 0{\cdot}05$) was performed for the values of magnesium release for all methods with every magnesium alloy tested with both electrolytes. The differences between the analyzed and calculated values for the magnesium release in PBS$^-$ were significant for all magnesium alloys tested. The magnesium releases of MgAl9 and MgAl3 were not significantly different between the calculated values in PBS$^-$ and in AP and in the comparison of the values analyzed/calculated in AP. The analyzed data values for MgAl3 and MgAl9Zn1 in AP were not significantly different. The differences in the values were significant for other alloys compared in the same groups. The calculated magnesium release based on the time of 900 s (calculation version 2) showed the expected lower values for all magnesium alloys in both electrolytes. But the same ranking could be found similar to the electrochemical parameters.

3.3 Zone coulometry of the anodic polarization measurements

The calculation of the electrical charges in milli-Coulomb per square centimeter for each trial can be observed in Figures 4–8 and were performed with each magnesium alloy and for both electrolytes. In general, differences in the calculated electrical charges can be observed between trials 1 and 2 compared with trials 3–5. The electrical charges from trials 1 and 2 were higher (maximum: 3000 mCb/cm^2) compared with trials 3–5 (maximum: 80 mCb/cm^2). Because the results of trials 3–5 concern the initial corrosion behavior, a ranking of the magnesium alloys could be created similar to that of the electrochemical parameters from the

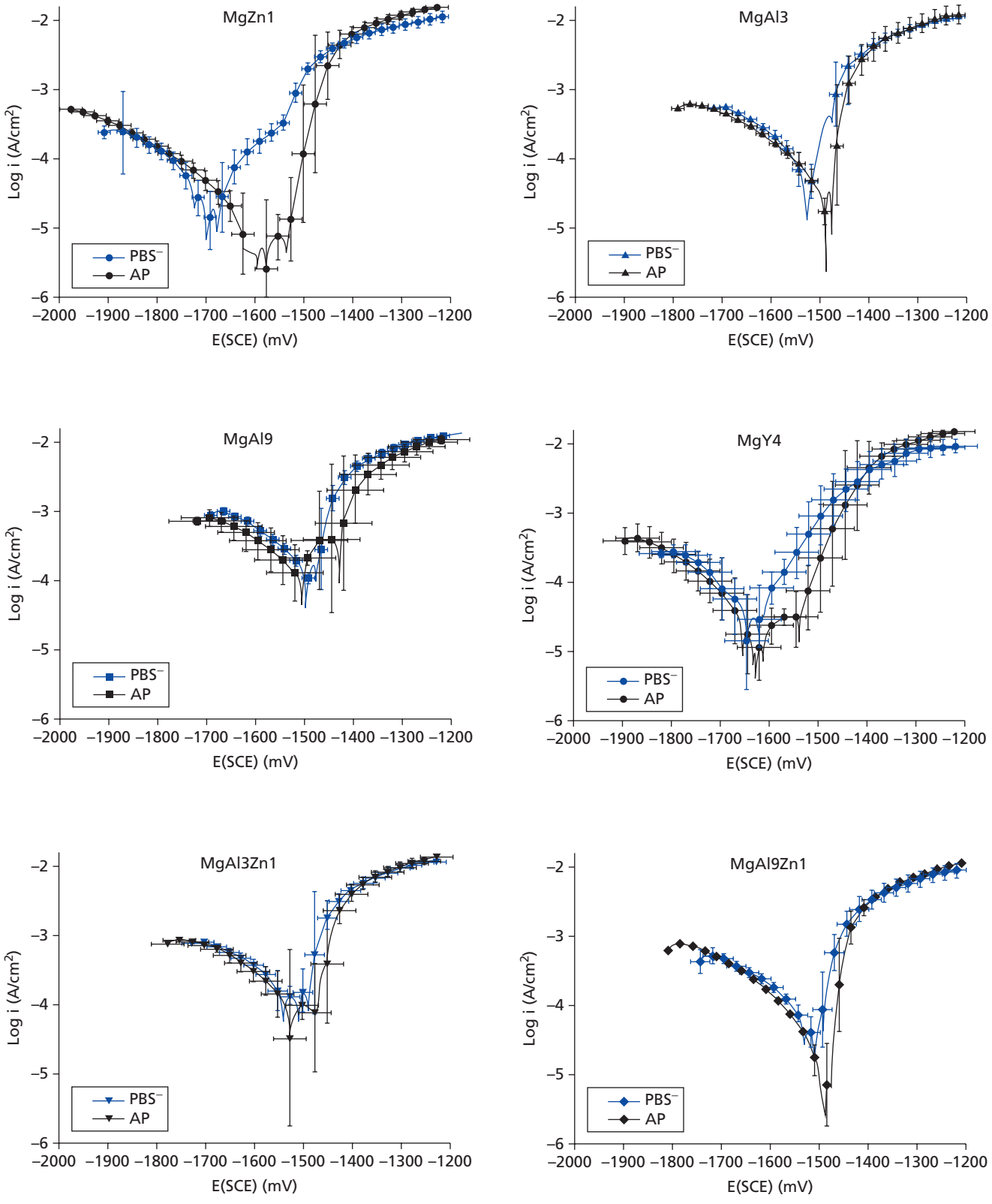

Figure 2. Anodic polarization plots for each magnesium alloy tested in each electrolyte.

anodic polarization plots for both electrolytes. This ranking was not applicable for trials 1 and 2 because the potential steps were too large. On the other hand, the rankings show the electrical charge over a large potential range of the anodic polarization plot. The anodic polarization plots in Figure 2 and the potential range E_z to –1400 mV show that the breakdown potentials for MgZn1

	i_{corr} (µA/cm²)	R_p (Ωcm²)	E_p (mV)	i_p (µA/cm²)	CR (mm/year)	E_z (mV)	Anodic immersion time (min)
PBS⁻							
Mg1Zn (*n* = 5)	47 ± 20	1129 ± 233	–1535 ± 6	386 ± 66	2·11 ± 0·89	–1693 ± 19	19·88 ± 0·31
Mg4Y (*n* = 5)	74 ± 22	835 ± 186	–1546 ± 5	472 ± 177	3·35 ± 1·00	–1642 ± 24	19·03 ± 0·41
Mg3Al (*n* = 5)	316 ± 102	217 ± 114	—	—	14·29 ± 4·61	–1513 ± 17	16·89 ± 0·28
Mg9Al (*n* = 6)	571 ± 209	86 ± 13	—	—	25·78 ± 9·43	–1484 ± 5	16·41 ± 0·09
Mg3AlZn1 (*n* = 4)	556 ± 44	141 ± 49	—	—	25·11 ± 1·98	–1507 ± 7	16·78 ± 0·12
Mg9AlZn1 (*n* = 6)	194 ± 96	317 ± 217	—	—	8·75 ± 4·33	–1511 ± 29	16·85 ± 0·48
AP							
Mg1Zn (*n* = 4)	7 ± 5	3913 ± 865	–1507 ± 10	21 ± 14	0·33 ± 0·24	–1582 ± 28	17·79 ± 0·13
Mg4Y (*n* = 5)	17 ± 12	1560 ± 429	–1500 ± 1	68 ± 20	0·75 ± 0·52	–1612 ± 11	18·54 ± 0·19
Mg3Al (*n* = 2)	45 ± 33	113 ± 77	—	—	2·02 ± 1·48	–1481 ± 3	16·35 ± 0·05
Mg9Al (*n* = 2)	160 ± 71	64 ± 13	—	—	7·21 ± 3·21	–1467 ± 4	16·12 ± 0·07
Mg3AlZn1 (*n* = 4)	145 ± 60	63 ± 37	—	—	6·55 ± 2·73	–1482 ± 3	16·36 ± 0·05
Mg9AlZn1 (*n* = 3)	19 ± 15	314 ± 202	—	—	0·87 ± 0·67	–1486 ± 2	16·43 ± 0·04

AP, artificial plasma; CR, corrosion rate; E_p, breakdown or pitting potential; E_z, zero potential; i_{corr}, corrosion current density; i_p, current density; PBS⁻, phosphate buffered saline; R_p, polarization resistance.

Table 3. Calculated results of the anodic polarization measurements in PBS⁻ and AP.

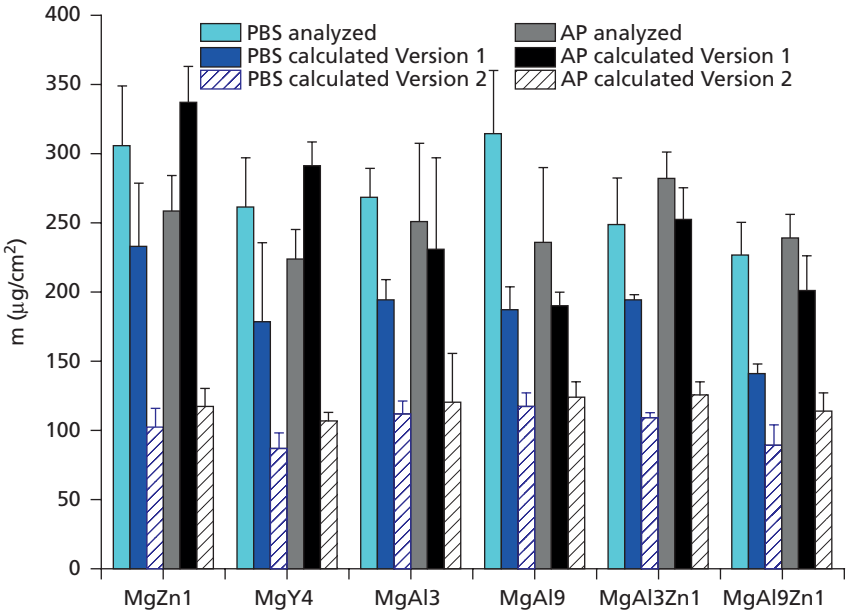

Figure 3. Comparison of magnesium-release (analyzed/calculated) from the anodic polarization measurements.

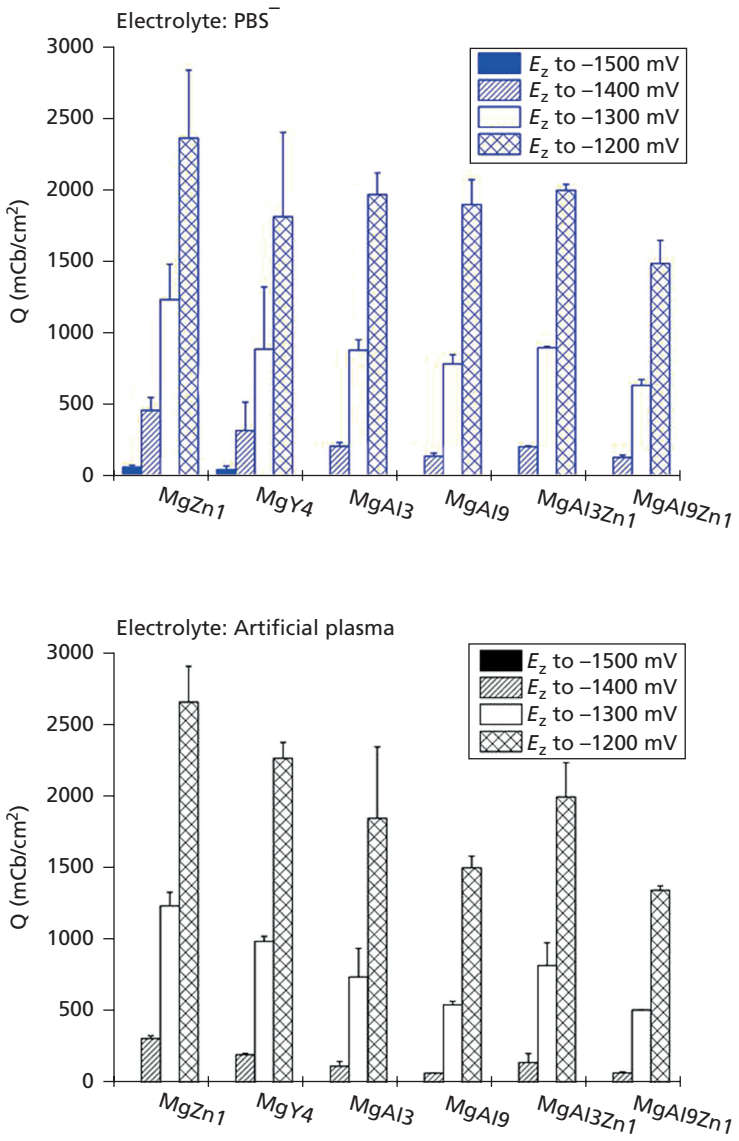

Figure 4. Calculated electrical charge (measured in milli-Coulomb per square centimeter) of each zone according to Maranche.

and MgY4 were already exceeded, and the current densities were between 3 and 8 mA/cm^2. The results from Figures 4 and 5 provide information about only the degradation process or the overall corrosion behavior and not specifically about the initial corrosion process.

4. Discussion

All of the magnesium alloys tested showed similar corrosion behavior in AP and PBS$^-$. However, lower corrosion values were observed in the AP. For both electrolytes, the alloys containing aluminum showed a non-breakdown potential; however, MgZn1 and MgY4 showed a smaller value. The magnesium alloys that were used in this study are experimental alloys. The alloys had a composition similar to those of the magnesium alloys on the market; however, they do not contain manganese. Manganese was not used to avoid complex alloys where it is not sure which alloying elements are responsible for a certain response. In Mg-Al alloys, a focus was layed on the influence of different amounts of aluminum and of 1 wt.% zinc. Therefore, binary Mg-(3,9)Al, Mg1Zn, and ternary Mg-(3,9)Al1Zn were chosen for this investigation, besides the binary Mg4Y (which is the base for WE43, an alloy that has been commercially used for stents). In general, low manganese contents are common in almost all Mg-Al alloys. In general, in

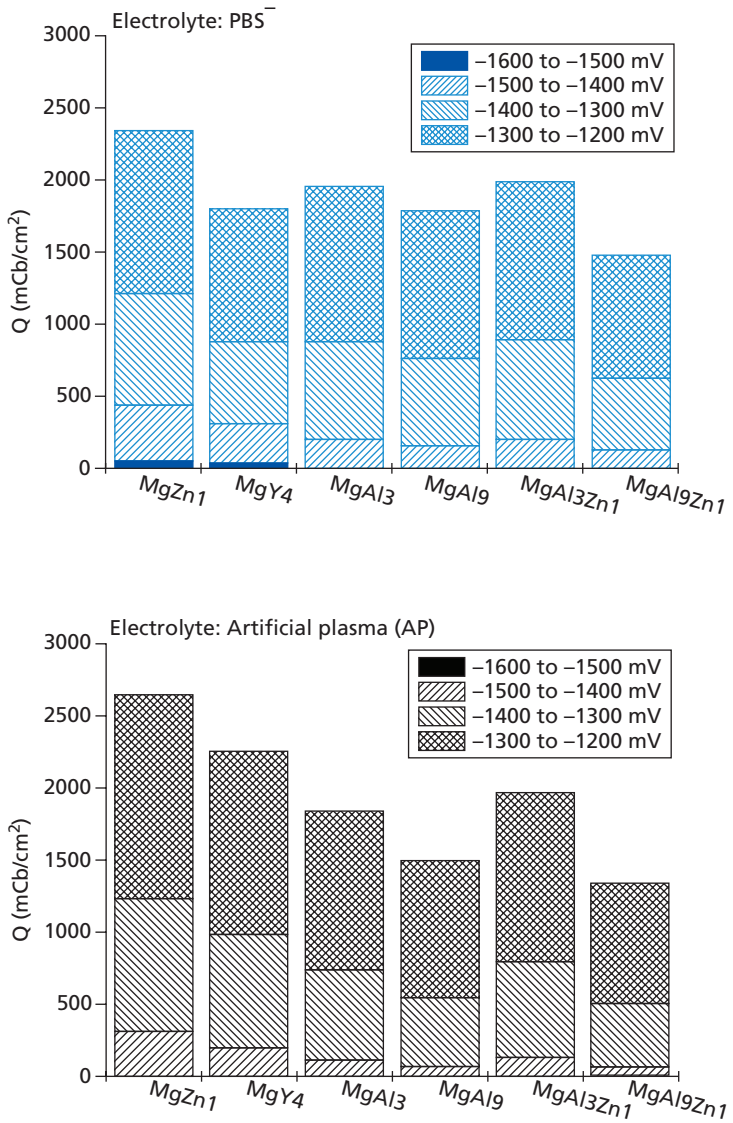

Figure 5. Calculation of the electrical charge (measured in milli-Coulomb per square centimeter) according to Reclaru.

aluminum-containing alloys, the Al-Mn intermetallics can be used to control the iron impurities because they form complex intermetallic phases to remove the iron from molten magnesium. These intermetallics are having a higher density and settle in the sludge. To a certain extend, manganese also improves ductility while having almost no influence the yield strength. Amounts larger 2 wt.% do not further improve the property profile in a positive manner.[25,26] Therefore, the alloys can be compared with AZ31 and AZ91.

For all of the measurements and calculations that were performed in this study, the magnesium alloy MgAl9Zn1 showed the lowest corrosion values of the tested magnesium alloys containing aluminum. In both electrolytes, the magnesium alloy MgAl9Zn1 attains values similar to those of MgZn1 and MgY4.

In this study, the influence of zinc on the magnesium alloys containing aluminum can be observed. In both electrolytes, the addition of zinc enhances the corrosion behavior of MgAl3Zn1 and MgAl9Zn1 compared with MgAl3 and MgAl9. In addition, the influence of zinc can be observed from the results of zone coulometry. In both electrolytes, with the exception of MgAl9Zn1, the magnesium alloys containing aluminum showed the highest calculated electrical charges, as shown in Figures 6–8. From the results of zone coulometry for the potential range near E_z, a division of the magnesium alloys similar to that for the

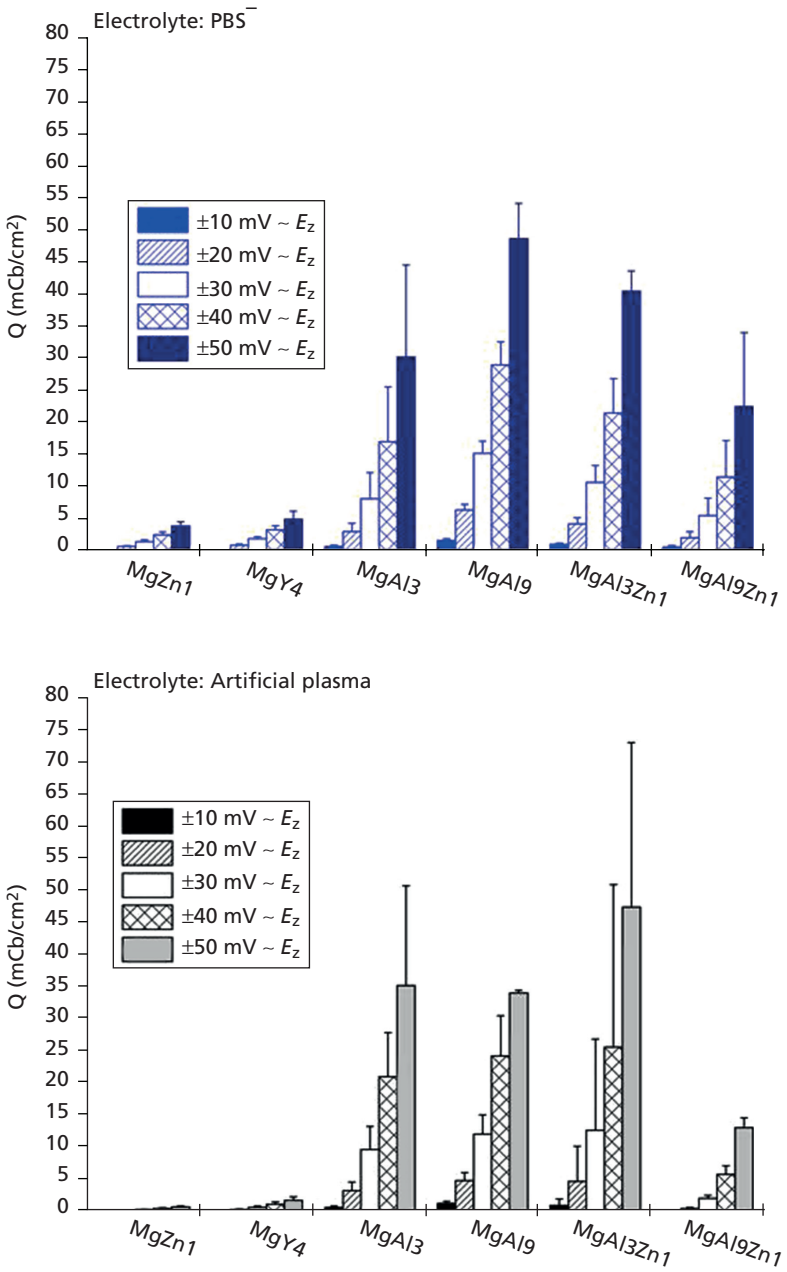

Figure 6. Electrical charge calculated stepwise from ±10 mV ~E_z to ±50 mV ~E_z.

electrochemical results of the anodic polarization measurements can be made. The results of Figures 6–8 show that with a potential range of 20 mV ~E_z, the calculated electrical charges strongly increase for MgAl3, MgAl3Zn1 and MgAl9 independent of the starting potential. The division of the potential ranges according to Figures 6–8 is not useful for MgZn1 and MgY4 because both alloys do not reach the breakdown potential at 40 mV ~E_z. Therefore, the chosen potential ranges from Figures 6–8 are useful for only magnesium alloys that showed no breakdown potential. The zone coulometric data according to Reclaru can be used for all magnesium alloys tested because the calculations were performed from −1600 mV up to −1200 mV (reference) in 100-mV steps. In general, the size of the calculated electrical charge depends on the current density and potential range of the passive range and the current increase during the breakdown potential. On the other hand, the calculated electrical charge depends on the time resulting from the scan rate used for the anodic polarization measurements. High electrical charges in a small potential range

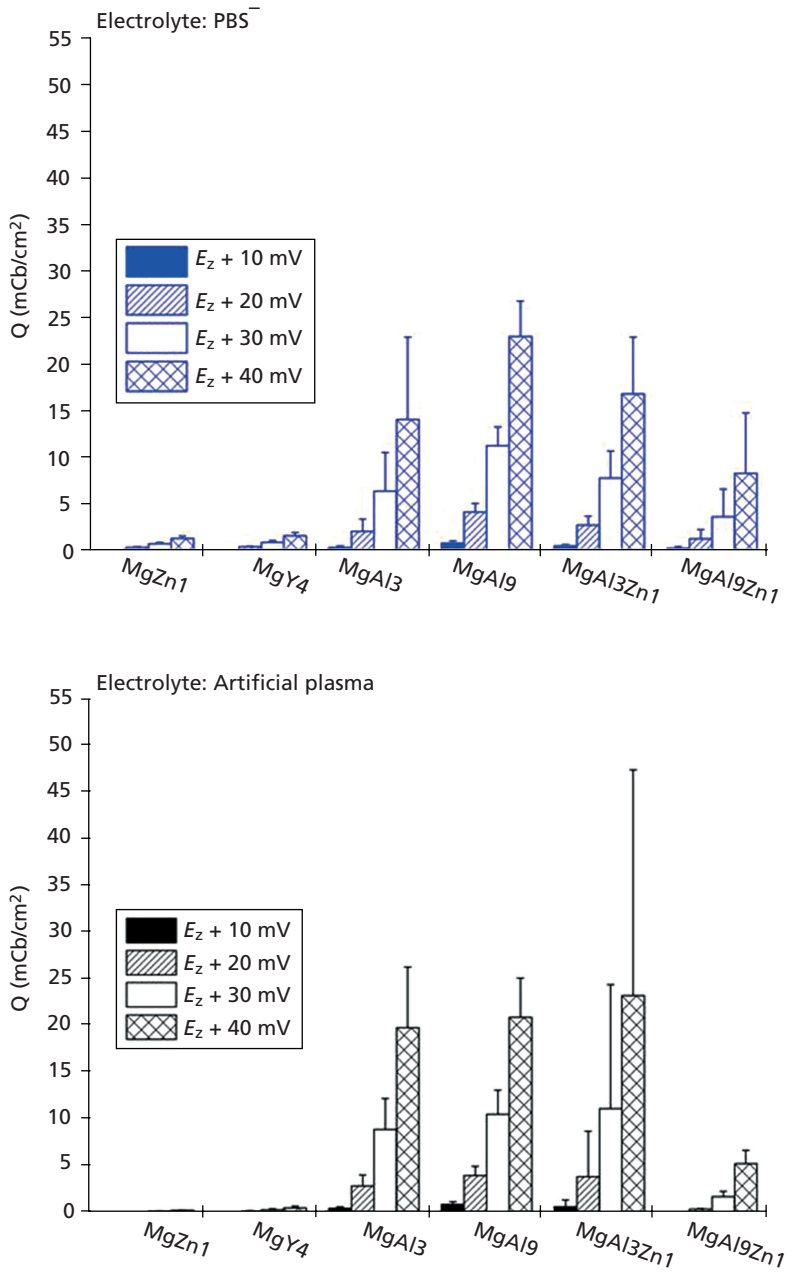

Figure 7. Electrical charge with E_z as the starting potential and increased stepwise from 10 to 40 mV.

mean high-current-density flow over a small period of time. The stepwise zone coulometry according to Reclaru is more accurate, and each potential range represents the corrosion state. Another advantage is that the comparison of the electrical charges using integration or the sum of all steps of the zone coulometry can be used to calculate the magnesium release using Faraday's law. The calculated magnesium release can be compared with the analyzed magnesium release. In this study, the magnesium releases after the anodic polarization measurements that were measured by ICP-OES and calculated by Faraday's law range from 141 to 335 µg/cm^2. The calculated values were lower in both electrolytes and generally lower in AP. The analytical magnesium release values showed a similar relationship for all magnesium alloys tested. A similar relationship for the electrochemical parameters could not be clearly determined. One reason could be the choice of the end potential, which was –500 mV. This end potential is higher than the degradation potential. Another reason could be the different anodic immersion times, which were calculated for

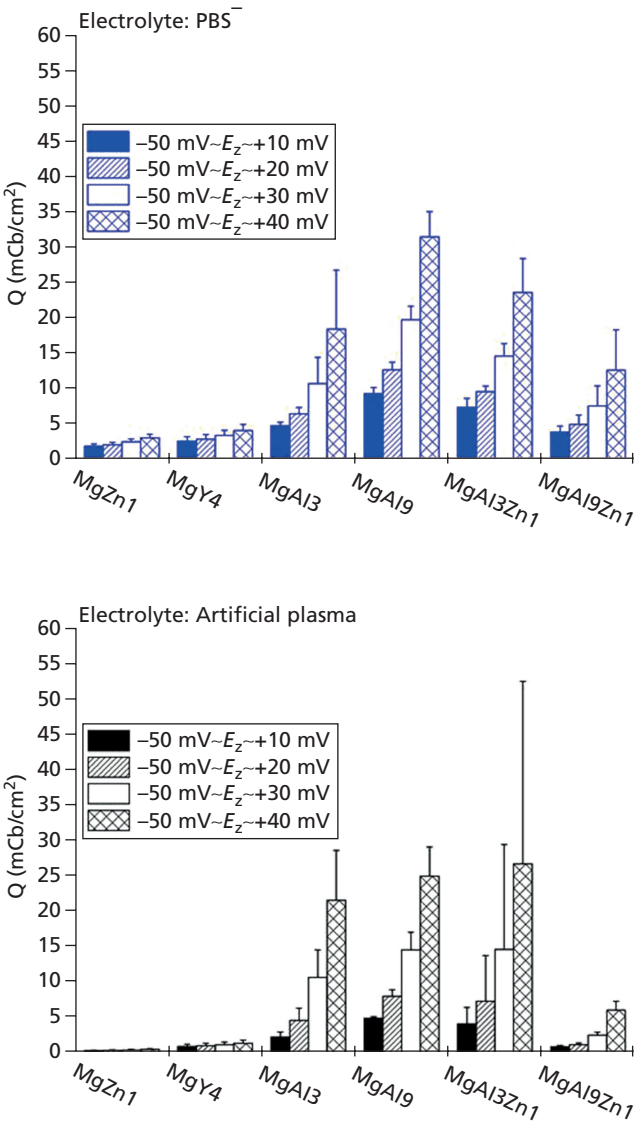

Figure 8. Electrical charge with –50 mV ~E_z as the starting potential and increased stepwise from 10 to 40 mV.

each magnesium alloy. These results can be seen in Table 3. The longest anodic immersion time was found for MgZn1 and MgY4 in both electrolytes. To eliminate the anodic immersion time, the mass loss according to Faraday was calculated with t = 900 s for all magnesium alloys tested, which can be seen in Figure 3 (calculation version 2). With this calculation, the calculated mass loss was lower for all magnesium alloys, but a same ranking could be found similar to the electrochemical data. Nagayama[12] found lower values for the calculated data compared with the measured values obtained using ICP-MS.

All analytical data of magnesium release from the anodic polarization measurements used in this study were similar. To classify the values of the analyzed magnesium release based on the degradation behavior, the values were compared with the mechanism for magnesium in the human body that is described in the review by Sarik *et al*.[27] In this study, the reference range for the total magnesium concentration in the adult blood plasma is reported to be 0·65–1·05 mmol/l. By calculating the analytical values from this study in terms of millimole per liter, the authors observed that the values are very low and beneath both limits. However, the dynamic immersions test that was performed in the human whole blood with these alloys for 6 h exceeded these limits.[28]

The degradation rate is typically measured using the hydrogen evolution test or the weight loss test. A magnesium sample is covered with an electrolyte or SBF, and the hydrogen evolution over time is measured. In addition, the weight loss or weight increase is measured, and the CR is calculated using the equation $CR = \Delta m / A \times t$, where A is the surface area of the sample, and t is the immersion time. However, many data have been reported concerning the degradation rate and its relationship to the type of electrolyte, choice of magnesium alloy, casting and surface conditions, immersion time and so on. Currently, there are no upper or lower limits for the degradation behavior of magnesium alloys concerning magnesium release. In contrast, the accepted corrosion behavior of dental alloys has strict limits. According to ISO 22674, the total mass loss after 7 d of immersion in artificial saliva must be less than 200 µg/cm².[27,29,30]

There are many SBF that can be used for *in vitro* corrosion testing.[1,5,29,30,31] Quach *et al*.[6] used AP that contained magnesium sulfate. In this investigation, PBS⁻ and AP were used as SBF. Both electrolytes contain no magnesium and the magnesium release can be measured. However, whether SBF is a good simulator of conditions in the human body remains to be determined. Corrosion measurements with the magnesium alloys used in this study showed different corrosion behaviors in human whole blood compared with those in PBS⁻.[28,32] For future *in vitro* corrosion studies, a SBF must be developed which is similar to human whole blood.[29] Several studies have shown that it is difficult to describe the corrosion behavior of magnesium alloys using anodic polarization measurements.[8,10] A study by Shi *et al*. did not show a good relationship between the calculated CRs from Tafel extrapolation and weight loss measurements. In another study, the Tafel plot measurements were performed with different immersion times before starting the Tafel plot measurements.[8] On the basis of these studies, a comparison between the calculated CRs from Tafel extrapolation and those from weight loss measurements is appropriate. In this study, the anodic polarization plots were started immediately without any immersion delay. To test if the CR can be calculated, additional diagrams ($1/R_p$–i_{corr} plots) were made according to Grajower and Greener[24] as shown in Figure 9. They showed linear behavior, which indicates the validity of the Stern-Geary approximation.[24]

These plots were made using the calculated results from the anodic polarization measurements. The conditions for calculating the CR were obtained from the linear behavior of the magnesium alloys as shown in Figure 9. Figure 9 shows a good linear relationship between i_{corr} and $1/R_p$ for the magnesium alloys MgZn1 and Mg4Y, which can be confirmed by $R^2 = 0{\cdot}907$. Hence, for these two alloys, the CR can be calculated for both electrolytes. The relationships for the other alloys were not sufficiently linear ($R^2 < 0{\cdot}55$). For these alloys measurements, such as weight loss are necessary. Therefore, the calculation of the CRs from the electrochemical polarization data is only partially useful. Furthermore, because the CR of the degradable magnesium alloys is not constant over time, the calculation of the CR for the short-term i_{corr} and R_p measurements is uncertain. Overall, it could be demonstrated that it is reasonable to apply and to test proven calculation techniques from corrosion studies using non-degradable alloys for the corrosion evaluation of magnesium alloys.

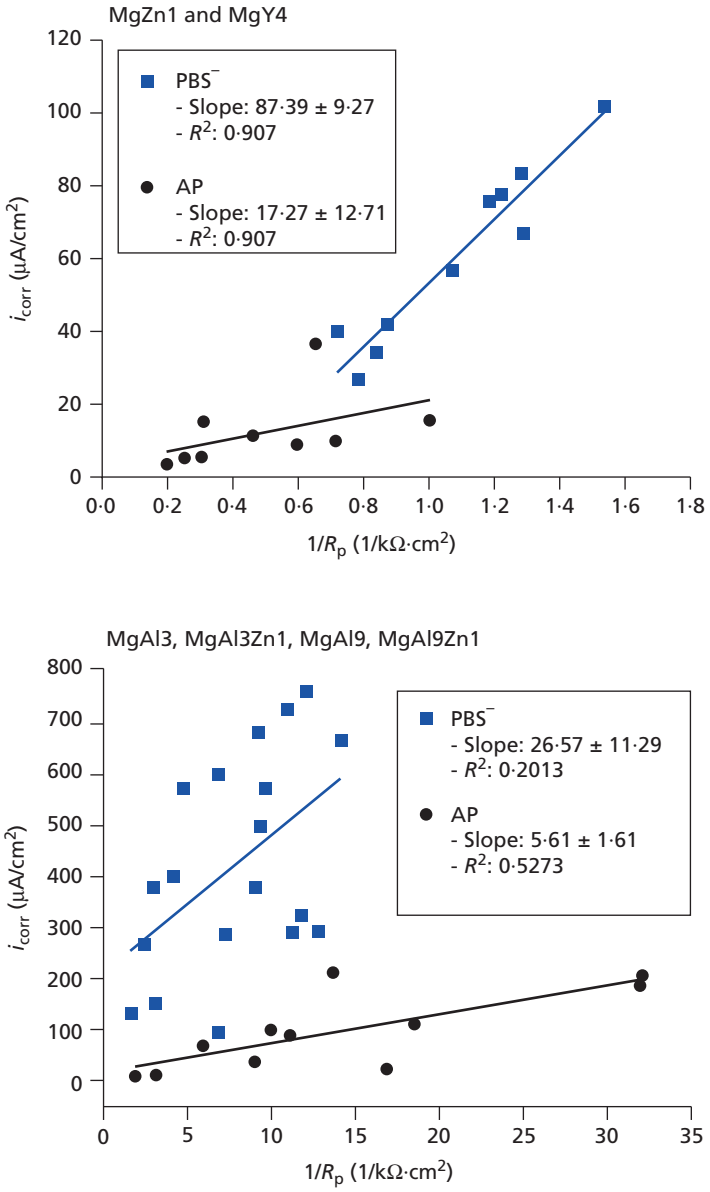

Figure 9. $1/R_p$–i_{corr} plots for MgZn1, MgY4, MgAl3, MgAl3Zn1, MgAl9 and MgAl9Zn1 in each electrolyte. Linear behavior indicates that the calculation of corrosion rate is reliable only for MgZn1 and MgY4 ($R^2 = 0{\cdot}907$).

5. Conclusion

The following conclusions can be made from the results of this study:

- The electrochemical corrosion measurements performed in this study show that all magnesium alloys tested showed higher corrosion resistance in AP than in PBS^- caused by less chloride contents and a higher pH. However, the ranking of the alloys is similar in both electrolytes.
- The calculated electrical charge and the calculated mass loss using Faraday's law provides additional information concerning the degradation behavior of the magnesium alloys tested. A good relationship was observed between the analyzed and calculated magnesium release.
- Performing zone coulometry according to Reclaru and Maranche[14–19] was possible. However, the choice of the potential regions must be in a small range (10–50 mV ~E_z) representing the initial corrosion behavior, which is relevant to clinical applications.
- The results from zone coulometry must be confirmed with other magnesium alloys and SBF.
- Zone coulometry used here can be considered as an additional corrosion test method for the evaluation of magnesium alloys.
- The experimental alloy MgAl9Zn1 can be used for further investigations as a bone-replacement material.
- These data from zone coulometry provide a better evaluation of the magnesium alloys than determination of magnesium release.
- In this study, the authors showed that the CR can be predicted from the results of anodic polarization measurements in case of linear $1/R_p$–i_{corr} relationship.

Acknowledgements

This study was supported by AiF (Project number: KF548101PK7).

REFERENCES

1. Liu, C. Degradation susceptibility of surgical magnesium alloy in artificial biological fluid containing albumin. *Journal of Materials Research* **2007**, *22*, 1806–1814.
2. Yfantis, C. D.; Yfantis, D. K.; Anastassopoulou, J.; Theophandes, T.; Staiger, M. *In vitro* corrosion behavior of new magnesium alloys for bone application. In *Proceedings of the 5th WSEAS International Conference on Environment, Ecosystems and Development*. Venice, 2006, 20–22.
3. Moravej, M.; Mantovani, D. Biodegradable metals for cardiovascular stent application: interests and new opportunities. *International Journal of Molecular Sciences* **2011**, *12*, 4250–4270.
4. Xin, Y.; Hu, T.; Chu, P. K. Influence of test solutions on *in vitro* studies of biomedical magnesium alloys. *Journal of The Electrochemical Society* **2008**, *157*, C238–C243.
5. Oyane, A.; Kim, H-M.; Furuya, T.; Kobubo, T.; Miyazaki, T. Preparation and assessment of revised simulated body fluids. *Journal of Biomedical Materials Research* **2003**, *65A*, 188–195.
6. Quach, N-C.; Uggowitzer, P.; Schmutz, P. Corrosion behavior of a Mg-Y-RE alloy used in biomedical applications studied by electrochemical techniques. *Comptes Rendus Chimie* **2008**, *11*, 1043–1054.
7. Schmutz, P.; Quach-Vu, N-C.; Gerber, I. Metallic medical implants: electrochemical characterization of corrosion processes. *The Electrochemical Society Interface* **2008**, *Summer*, 35–40.
8. Shi, Z.; Atrens, A. An innovative specimen configuration for the study of Mg corrosion. *Corrosion Science* **2011**, *53*, 7–25.
9. *DIN EN ISO 10271: Dental Metallic Materials – Corrosion Test Methods*. Berlin: Beuth Verlag, 2002.
10. Shi, Z.; Liu, M.; Atrens, A. Measurement of the corrosion rate of magnesium alloys using Tafel extrapolation. *Corrosion Science* **2010**, *52*, 579–588.
11. Song, G. Control of biodegradation of biocompatible magnesium alloys. *Corrosion Science* **2007**, *49*, 1696–1701.
12. Nakayama, Y. Anodic polarization measurements of orthopaedic implant alloys in bovine serum albumin. *Journal of Applied Biomaterials & Functional Materials* **1990**, *1*, 307–313.
13. Schille, C.; Hausch, G.; Schweizer, E.; Geis-Gerstorfer, J. *57. Jahrestagung der DGZPW Wuppertal*, **2008**.
14. Maranche, C.; Hornberger, H. A proposal for the classification of dental alloys according to their resistance to corrosion. *Dental Materials* **2007**, *23*, 1428–1437.
15. Reclaru, L.; Meyer, J-M. Zonal coulometric analysis of the corrosion resistance of dental alloys. *Journal of Dentistry* **1995**, *23*, 301–311.
16. Reclaru, L.; Lerf, R.; Eschler, P-Y.; Blatter, A.; Meyer, J-M. Evaluation of corrosion on plasma sprayed and anodized titanium implants, both with and without bone cement. *Biomaterials* **2003**, *24*, 3027–3038.
17. Reclaru, L.; Lüthy, H.; Ziegenhagen, R.; Eschler, P-Y.; Blatter, A. Anisotropy of nickel release and corrosion in austenitic stainless steels. *Acta Biomaterialia* **2008**, *4*, 680–685.
18. Reclaru, L.; Eschler, P-Y.; Lerf, R.; Blatter, A. Electrochemical corrosion and metal ion release from Co-Cr-Mo-prosthesis with titanium plasma spray coating. *Biomaterials* **2005**, *26*, 4747–4756.
19. Mareci, D.; Chelariu, R.; Gordin, D-M.; Ungureanu, G.; Gloriant, T. Comparative corrosion study of Ti-Ta alloys for dental applications. *Acta Biomaterialia* **2009**, *5*, 3625–3639.
20. Mueller, W-D.; Fernandez Lorenzo de Mele, M.; Nascimento, M. L.; Zeddies, M. Degradation of magnesium and its alloys: dependence on the composition of the synthetic biological media. *Journal of Biomedical Materials Research* **2009**, *90A*, 487–495.

21. Kirkland, N. T.; Espagnol, J.; Birbilis, N.; Staiger, M. P. A survey of bio-corrosion rates of magnesium alloys. *Corrosion Science* **2010**, *52*, 287–291.
22. Schille, C.; Braun, M.; Wendel, H-P.; Scheideler, L.; Hort, N.; Reichel, H-P.; Schweizer, E.; Geis-Gerstorfer, J. Corrosion of experimental magnesium alloys in blood in PBS: a gravimetric and microscopic evaluation. *Materials Science and Engineering B* **2011**, *176*, 1797–1801.
23. *ASTM G5-87. Standard Reference Test Method for Making Potentiostatic and Potentiodynamic Anodic Polarization Measurements: ASTM 2004*. See www.astm.org for further details.
24. Grajower, R.; Greener, E. H. Corrosion currents of dental amalgams. *Journal of Biomedical Materials Research* **1980**, *14*, 547–556.
25. Emley, E. F. *Principles of Magnesium Technology*. Oxford: Pergamon Press, 1966.
26. Avedesian, M. M.; Baker, H. *ASM Specialty Handbook Magnesium*. Materials Park: ASM International, 1999.
27. Saris, N-E. L.; Mervaala, E.; Karppanen, H.; Khawaja, J. A.; Lewenstam, A. Review magnesium: an update on physiological, clinical and analytical aspects. *Clinica Chimica Acta* **2000**, *294*, 1–26.
28. Geis-Gerstorfer, J.; Schille, C.; Schweizer, E.; Rupp, F.; Scheideler, L.; Reichel, H-P.; Hort, N.; Nolte, A.; Wendel, H-P. Blood triggered corrosion of experimental magnesium alloys. *Material Science & Engineering B* **2011**, *176*, 1761–1766.
29. Xin, Y.; Hu, T.; Chu, P. K. *In vitro* studies of biomedical magnesium alloys in simulated physiological environment: a review. *Acta Biomaterialia* **2011**, *7*, 1452–1459.
30. *DIN EN ISO 22674: Dentistry-Metallic Materials for Fixed and Removable Restorations and Appliances*. Berlin: Beuth Verlag, 2006.
31. Kannan, M. B.; Sing, R. K. A mechanistic study of *in vitro* degradation of magnesium alloy using electrochemical techniques. *Journal of Biomedical Materials Research Part B* **2010**, *93A*, 1050–1055.
32. Schille, C.; Reichel, H-P.; Hort, N.; Geis-Gerstorfer, J. Corrosion of experimental magnesium alloys for use as a possible bone replacement material. In *Magnesium* (Kainer, K. (ed.)). Weinheim: Wiley, 2009, 1195–1200.